

Article

Dynamics of Coarse Woody Debris Characteristics in the Qinling Mountain Forests in China

Jie Yuan ¹ , Shibu Jose ², Xiaofeng Zheng ¹, Fei Cheng ^{1,3}, Lin Hou ^{1,4}, Jingxia Li ^{1,5} and Shuoxin Zhang ^{1,4,*}

¹ College of Forestry, Northwest A&F University, Yangling 712100, China; yuanjie@nwsuaf.edu.cn (J.Y.); xfzheng1991@gmail.com (X.Z.); feicheng@gxu.edu.cn (F.C.); houlin1969@163.com (L.H.); shuyaozhou2012@126.com (J.L.)

² School of Natural Resources, University of Missouri, Columbia, MO 65211, USA; joses@missouri.edu

³ Forestry College, Guangxi University, Nanning 530004, China

⁴ Qinling National Forest Ecosystem Research Station, Huoditang, Ningshan 711600, China

⁵ Gansu Forestry Technological College, Tianshui 741020, China

* Correspondence: sxzhang@nwsuaf.edu.cn; Tel./Fax: +86-29-87082993

Received: 15 September 2017; Accepted: 20 October 2017; Published: 23 October 2017

Abstract: Coarse woody debris (CWD) is an essential component in defining the structure and function of forest ecosystems. Long-term dynamics of CWD characteristics not only affect the release rates of chemical elements from CWD, but also the species diversity of inhabiting plants, animals, insects, and microorganisms as well as the overall health of ecosystems. However, few quantitative studies have been done on the long-term dynamics of CWD characteristics in forest ecosystems in China. In this study, we conducted nine tree censuses between 1996 and 2016 at the Huoditang Experimental Forest in the Qinling Mountains of China. We quantified forest biomass including CWD and CWD characteristics such as decay states and diameter classes during this period and correlated with stand, site, and climatic variables. The forest biomass was dominated by live tree biomass (88%); followed by CWD mass (6%–10%). Understory biomass contributed only a small portion (1%–4%) of the overall biomass. Significant differences in average annual increment of CWD mass were found among forest stands of different species ($p < 0.0001$). Forest biomass, stand age, forest type, aspect, slope, stand density, annual average temperature, and precipitation were all significantly correlated with CWD mass ($p < 0.05$), with forest type exhibiting the strongest correlation ($r^2 = 0.8256$). Over time, the annual mass of different CWD characteristics increased linearly from 1996–2016 across all forest types. Our study revealed that forest biomass, including CWD characteristics, varied by forest type. Stand and site characteristics (forest biomass, forest type, aspect, slope and stand density) along with temperature and precipitation played a major role in the dynamics of CWD in the studied forest ecosystems.

Keywords: coarse woody debris; biomass; forest management; redundancy analysis; characteristics dynamics; Qinling Mountains

1. Introduction

Coarse woody debris (CWD) is often removed from the forest floor with the intention of avoiding forest health issues such as insect and pest infestations, and to reduce flammable material with respect to forest fires [1]. However, CWD is critical in enhancing forest productivity [2], promoting forest restoration and natural regeneration after harvesting, and maintaining the stability and balance of forest biodiversity [3–5]. Thus, ecologists are paying increasing attention to the ecological functions of CWD in the forest ecosystem and its implications for forest management [6]. CWD has a high

ecological relevance and contributes significantly to critical ecological processes in carbon pools [7,8], biodiversity [9–12], and geomorphological stability [13].

Forest biomass is the foundation of research into many forestry and ecology problems, and is also a basic quantity character of the forest ecological system. Long-term monitoring of the dynamics of forest biomass can acquire accurate data that is vital for forest management, monitoring, and evaluation, and is also crucial for the terrestrial carbon cycle. As an indispensably important constituent of forest biomass, CWD is particularly under studied [14] and field observations are needed to support terrestrial carbon cycle modelling efforts [15]. CWD may be accounted for 20% of total carbon in primary (that is, old growth) [16] and secondary [17] forests. A key component in describing forest carbon dynamics is the change in CWD mass through time. The long-term dynamics of CWD may be reflected in the diversity of wood (for example, species, size, and stage of decay) and site attributes (for example, climate) across the study region [18]. Meanwhile, the analysis of the relationship between CWD mass and forest biomass is also significant. In the past two decades, CWD dynamics have been intensively studied in various forest ecosystems around the world where studies have focused on the stocks, dynamics of decomposition, and nutrient content of CWD [19–23]. However, few quantitative studies have been done on the long-term dynamics of the CWD mass in forest ecosystems [24,25], especially on the long-term dynamics of CWD characteristics (i.e., CWD composition including log, snag and stump, decay classes, and diameter classes). The precise understanding of CWD characteristics is the basis of CWD research, and is beneficial for revealing the relationship between the structure and function of CWD. The long-term dynamics of CWD characteristics not only affect the release rates of chemical elements from the CWD, but also influence the diversity of attached vegetation, insects, and microorganisms in CWD. Important insights into CWD dynamics have been gained by linking stand assessments to CWD characteristics, which are recognized to be a reflection of the past and present stand features to some extent [26,27].

The amount of CWD in an ecosystem is the balance of tree mortality and the decomposition. CWD input can be generated under situations of mortality resulting from competition among trees, natural death of the forest at the old stage, natural interferences (wind, rain, snow, fire, lightning, insect, debris flow, invasion of fungi, etc.), and human disturbances (e.g., thinning and final harvesting) [28–30]. The decomposition of CWD is caused by respiration, leaching, and fragmentation. Overall, the characteristics of CWD are a complex process, which depend on many factors (natural interferences, human disturbances, stand and site characteristics, and environmental conditions) derived from CWD input and decomposition. Unfortunately, the effects of most of these factors (forest biomass, stand age, forest type, altitude, aspect, slope, stand density, annual average temperature, and precipitation) are known only qualitatively, or from laboratory tests [31] as it is difficult to evaluate the effects of these factors on CWD characteristics due to the combined effect of multiple causes, which were studied short-term, fragmentary, and scattered in the past. Therefore, the long-term monitoring can acquire the multiple effect factors on CWD characteristics, which is necessary to reveal the reasons for the accumulation of CWD.

In China, the Qinling Mountains are an important climate boundary between subtropical and warm temperate zones where the typical vegetation of both climate zones assembles together with a high biodiversity [32]. However, in recent decades, the Huoditang Forest Region in the Qinling Mountains has been constantly affected by extreme weather (strong winds), insects and diseases (*Dendroctonus armandi*), resulting in increases in the quantity of CWD of the main species *Pinus armandi* (*P. armandi*) and *Quercus aliena* var. *acuteserrata* (*Q. aliena* var. *acuteserrata*).

In this study, we established permanent plots (*P. armandi*, *Q. aliena* var. *acuteserrata* forests, and mixed forests of the two species) to study CWD dynamics from a long-term project (1996–2016) at the Qinling National Forest Ecosystem Research Station (QNFERS). The objectives of this study were to: (1) compare the dynamics of forest biomass in the three forest types over a 20-year-period, and discuss the relationship between CWD mass and forest biomass; (2) quantify the dynamics of CWD characteristics in detail; and (3) assess the influence of stand, site, and climatic factors on the size and character of the CWD pool.

2. Materials and Methods

2.1. Study Area

Our study was conducted at the Huoditang Experimental Forest of Northwest A&F University in the Qinling Mountains, Shaanxi Province, China, which covers an area of 2037 ha. The altitude is 800–2500 m above sea level, the geographic coordinates are 33°18′–33°28′ N in latitude and 108°21′–108°39′ E in longitude. The annual average temperature is 10.50 °C, the mean annual precipitation is 1000 mm, the frost-free period is 170 days, and the climate is warm temperate. The abrupt and broken topography consists mainly of granite and gneiss. The mean soil depth is 45 cm. The soil units are cambisols, umbrisols, and podzols.

The study area underwent intensive selective logging in the 1960s and 1970s; however, since then there have been no significant anthropogenic disturbances, except for lacquer tree tapping and occasional illegal tree felling. Since the natural forest protection project was initiated in 1998, anthropogenic disturbance of any kind has been absent in the region. In this study, the investigated forests were natural secondary forests, all 40 years old in 1996. The *P. armandi* forest was dominated by *P. armandi* (80% of trees), with a forest canopy density of 65%. The mean stand height and diameter at breast height (DBH, measured at 1.3 m above ground level) were 14 m and 21 cm, respectively. In the shrub layer, height varied from 25 cm to 410 cm and the percent cover was 28%. The major shrubs species present were *Euonymus phellomanus* (*E. phellomanus*), *Symplocos paniculata* (*S. paniculata*), *Spiraea wilsonii*, *Litsea tsinlingensis* (*L. tsinlingensis*) and *Schisandra sphenanthera* (*S. sphenanthera*), together with herbs, e.g., *Carex leucochlora* (*C. leucochlora*), *Lysimachia christinae*, *Rubia cordifolia*, *Houttuynia cordata*, *Pinellia ternata* (*P. ternata*), *Sedum aizoon* (*S. aizoon*), and ferns. The average height of the herbs was 28 cm and the percent cover was 35%. The *Q. aliena* var. *acuteserrata* forest was dominated by *Q. aliena* var. *acuteserrata* (85% of trees), with a forest canopy density of 75%. The mean stand height and DBH were 12 m and 18 cm, respectively. In the shrub layer, height varied from 45 cm to 650 cm and the percent cover was 25%. The major shrubs species present were *Lonicera hispida* (*L. hispida*), *Sinarundinaria nitida* (*S. nitida*), *S. paniculata*, *Lespedeza buergeri* and *Rubus pungens* (*R. pungens*), together with herbs, e.g., *Spodiopogon sibiricus* (*S. sibiricus*), *Epimedium brevicornu* (*E. brevicornu*), *Daphne tangutica* (*D. tangutica*), *Urtica fissa*, *Paris quadrifolia*, and *Pteridophyta*. The average height of the herbs was 35 cm and the percent cover was 30%. The mixed forest was dominated by *Q. aliena* var. *acuteserrata* (40% of trees) and *P. armandi* (50% of trees), with a forest canopy density of 70%. The mean stand height and DBH were 14 m and 20 cm, respectively. In the shrub layer, height varied from 35 cm to 520 cm and the percent cover was 32%. The major shrubs species present were *L. hispida*, *S. nitida*, *S. paniculata*, *L. tsinlingensis*, *R. pungens*, *E. phellomanus* and *S. sphenanthera*, together with herbs, e.g., *S. sibiricus*, *E. brevicornu*, *D. tangutica*, *C. leucochlora*, *P. ternata*, *S. aizoon*, and ferns. The average height of the herbs was 42 cm and the percent cover was 35%.

2.2. Field Sampling

In the summer of 1996, we selected *P. armandi*, *Q. aliena* var. *acuteserrata* forests and a mixed forest of *Q. aliena* var. *acuteserrata* and *P. armandi* for our permanent plots, and randomly established six sample plots with an area of 60 m × 60 m in each of the forest types (Figure 1, Table 1). To reduce disturbance, these sample plots were protected by an enclosure. Each sample plot was located at least 50 m from the forest edge and was separated from other plots by a buffer strip of at least 100 m. We assumed that the annual average precipitation was the same in these sample plots in a year. The annual average temperature and precipitation during 1996–2016 are shown in Figure 2, which were measured from a HMP45C weather station (Vaisala, Helsinki, Finland) located 1612 m above sea level in this region (33°20′16″ N and 108°26′45″ E). We also assumed a standard lapse rate of 0.7 °C in this forest area, and estimated the annual average temperatures in these sample plots.

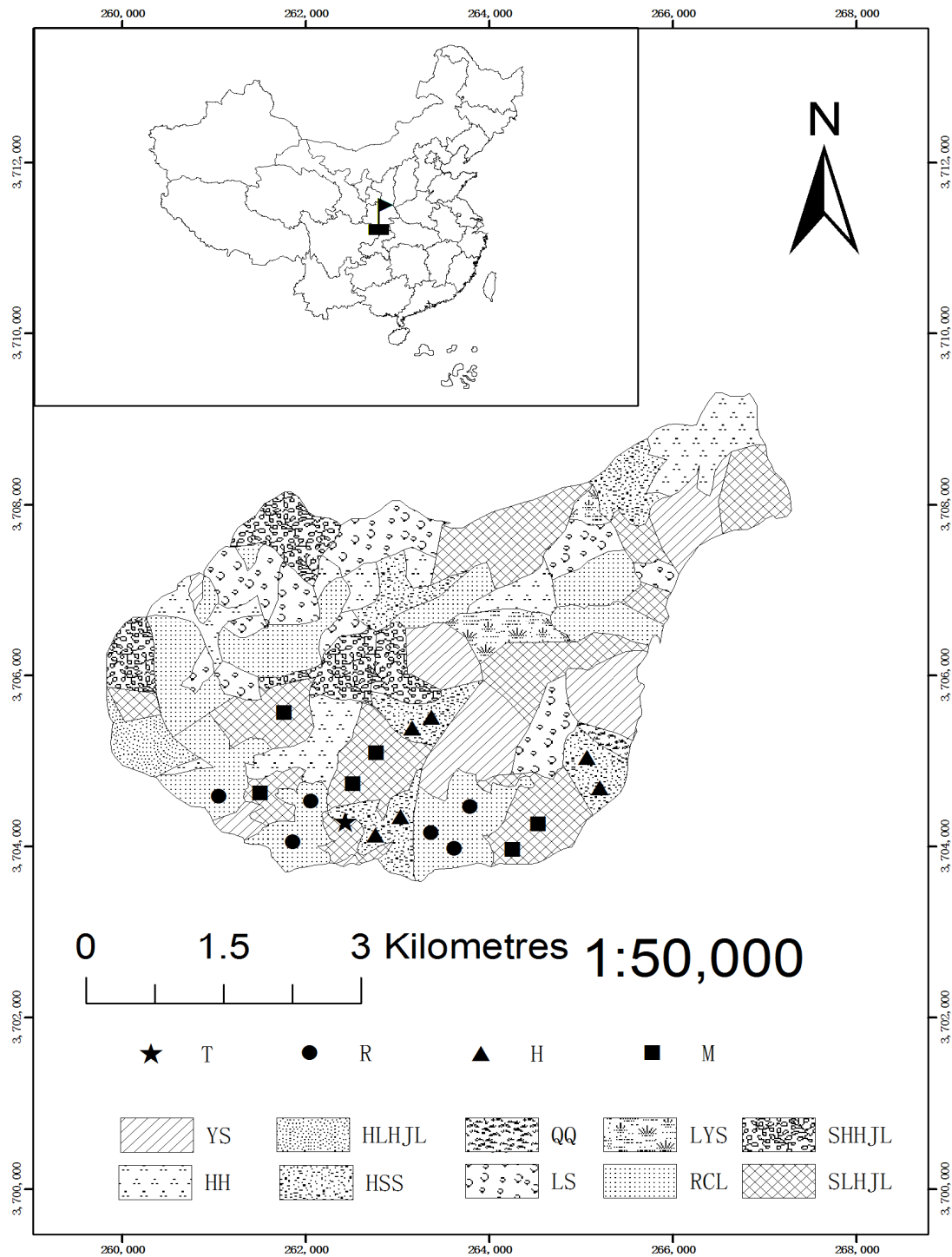


Figure 1. Location of the plots for *P. armandi*, *Q. aliena* var. *acuteserrata* forests and a mixed forest of *Q. aliena* var. *acuteserrata* and *P. armandi* on the Huoditang Experimental Forest Farm in the Qinling Mountains (China). T = Weather station; R = Plots in *Q. aliena* var. *acuteserrata* forest; H = Plots in *P. armandi* forest; M = Plots in mixed forest of *Q. aliena* var. *acuteserrata* and *P. armandi*; YS = *Pinus tabulaeformis* forest; HLHJL = Mixed forest of *Q. aliena* var. *acuteserrata* and *Betula albo-sinensis*; QQ = *Picea wilsonii* forest; LYS = *Larix principis-rupprechtii* forest; SHHJL = Mixed forest of *P. armandi* and *B. albo-sinensis*; HH = *B. albo-sinensis* forest; HSS = *P. armandi* forest; LS = *Picea asperata* forest; RCL = *Q. aliena* var. *acuteserrata* forest; and SLHJL = Mixed forest of *Q. aliena* var. *acuteserrata* and *P. armandi*.

Table 1. Plot characteristics in the main types of forests in the Huoditang Experimental Forest Farm in the Qinling Mountains (China).

Sample Plots	Litter Horizons			Soil Type	Latitude and Longitude	Altitude (m)	Aspect	Slope	Stand Density (Trees·ha ⁻¹)
	Oi	Oe	Oa						
<i>Q. aliena</i> var. <i>acuteserrata</i> 1#	51%	23%	26%	mountain brown earth	33°20'55" N 108°23'54" E	1597	318°	32°	1183
<i>Q. aliena</i> var. <i>acuteserrata</i> 2#	54%	21%	25%	dark brown earth	33°19'20" N 108°25'48" E	1641	14°	28°	1482
<i>Q. aliena</i> var. <i>acuteserrata</i> 3#	52%	25%	23%	mountain brown earth	33°20'49" N 108°25'58" E	1620	277°	26°	1232
<i>Q. aliena</i> var. <i>acuteserrata</i> 4#	56%	21%	23%	mountain brown earth	33°19'10" N 108°28'48" E	1640	260°	23°	1024
<i>Q. aliena</i> var. <i>acuteserrata</i> 5#	53%	20%	27%	dark brown earth	33°20'08" N 108°28'12" E	1671	240°	30°	1086
<i>Q. aliena</i> var. <i>acuteserrata</i> 6#	52%	25%	23%	mountain brown earth	33°20'42" N 108°29'21" E	1534	218°	18°	1584
<i>P. armandi</i> 1#	58%	31%	11%	mountain brown earth	33°19'26" N 108°27'10" E	1410	288°	34°	1628
<i>P. armandi</i> 2#	61%	28%	11%	mountain brown earth	33°19'30" N 108°27'54" E	1460	198°	32°	1486
<i>P. armandi</i> 3#	61%	25%	14%	mountain brown earth	33°22'54" N 108°28'02" E	1483	245°	27°	1712
<i>P. armandi</i> 4#	57%	28%	15%	mountain brown earth	33°23'10" N 108°28'10" E	1532	194°	22°	1426
<i>P. armandi</i> 5#	62%	24%	14%	mountain brown earth	33°21'10" N 108°32'39" E	1540	243°	29°	1267
<i>P. armandi</i> 6#	60%	23%	17%	dark brown earth	33°22'01" N 108°32'19" E	1983	245°	15°	1834
Mixed forest 1#	54%	18%	28%	dark brown earth	33°22'24" N 108°27'10" E	1580	257°	22°	1354
Mixed forest 2#	48%	26%	26%	mountain brown earth	33°19'01" N 108°30'24" E	1481	204°	24°	1288
Mixed forest 3#	50%	24%	26%	mountain brown earth	33°20'10" N 108°30'42" E	1424	255°	32°	1078
Mixed forest 4#	52%	23%	25%	mountain brown earth	33°21'05" N 108°24'48" E	1582	73°	26°	1041
Mixed forest 5#	46%	22%	32%	dark brown earth	33°21'20" N 108°26'50" E	1798	182°	31°	1121
Mixed forest 6#	48%	24%	28%	dark brown earth	33°23'18" N 108°25'40" E	1627	202°	21°	1311

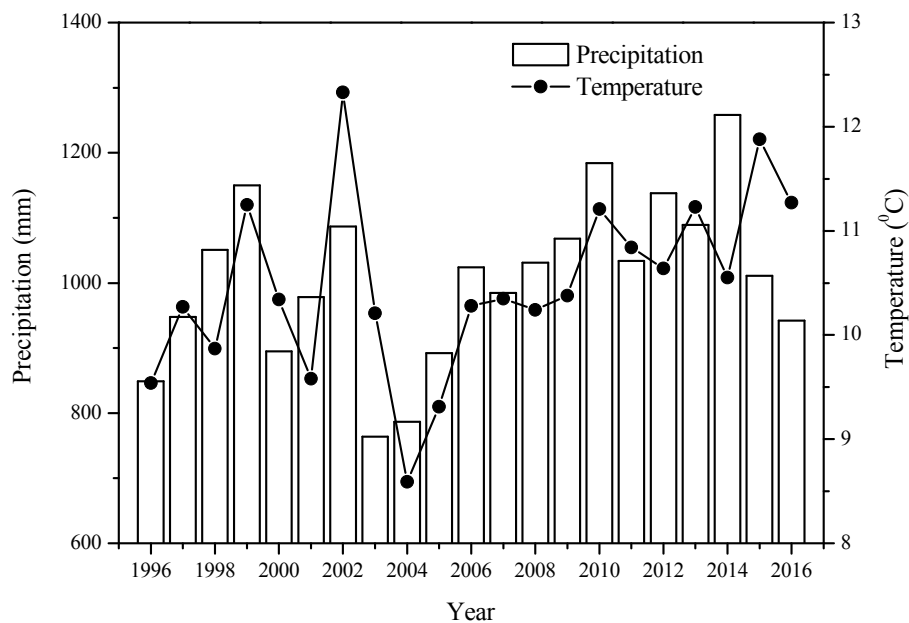


Figure 2. The variation in the mean annual temperature and total precipitation in the Huoditang forest region from 1996–2016. The data were sourced from the unpublished Qinling long-term ecological monitoring database.

We used the USDA Forest Service and Long Term Ecological Research (LTER) definition of CWD (diameter ≥ 10 cm at the widest point) [33]. CWD was categorized into logs, snags, and stumps as per Reference [34]: downed or leaning deadwood ($>45^\circ$ from vertical) with a minimum diameter ≥ 10 cm at the widest point and length ≥ 1 m was defined as a log; deadwood $\leq 45^\circ$ from vertical with a diameter at the widest point ≥ 10 cm was defined as a snag; and deadwood $\leq 45^\circ$ from vertical with a height ≤ 1 m and diameter ≥ 10 cm at the widest point was defined as a stump. Each piece of CWD was assigned to one of five decay classes on the basis of discrepancies in internal and external tissue characteristics (Table 2) [27]. The numbers 1–5 represent different decomposition stages where 1 represents the initial stage and 5 represents the final stage. In our study, CWD characteristics were CWD composition, decay classes, and diameter classes. CWD composition included log, snag, and stump; CWD decay classes were assigned from one to five; and CWD diameter classes contained four kinds (10–20 cm, 20–30 cm, 30–40 cm, and >40 cm).

The first forest survey to determine live and CWD mass was conducted in July of 1996. Eight more forest censuses were conducted in July of 1998, 2001, 2003, 2006, 2009, 2011, 2014, and 2016, giving a total of nine censuses during this 20-year study.

Table 2. Coarse woody debris (CWD) characteristics of different decay classes in a forest system.

Type	Characteristics	Decay Class				
		I	II	III	IV	V
Snags	Leaves	Present	Absent	Absent	Absent	
	Bark	Tight	Loose	Partly present	Absent	
	Crown, branch, and twig	All present	Only branches present	Only large branch stub present	Absent	As logs
	Bole	Recently dead	Standing, firm	Standing, decayed	Heavily decayed, soft, and block structure	
	Indirect measure	Cambium still fresh, died less than 1 year	Cambium decayed, knife blade penetrates a few millimeters	Knife blade penetrates less than 2 cm	Knife blade penetrates 2–5 cm	Knife blade penetrates all the way
Logs	Structure integrity	Sound	Sapwood slightly rotting, heartwood sound	Sapwood missing, heartwood mostly sound	Heartwood decayed	Soft
	Leaves	Present	Absent	Absent	Absent	Absent
	Branches	All twig present	Larger twig present	Larger branches present	Branch stubs present	Absent
	Bark	Present	Present	Often present	Often absent	Absent
	Bole shape	Round	Round	Round	Round to oval	Oval to flat
	Wood consistency	Solid	Solid	Semisolid	Partly soft	Fragmented to powdery
	Color of wood	Original color	Original color	Original color to faded	Original color to faded	Heavily faded
	Position of log on ground	Elevated on support point	Elevated on support point	Near or on ground	All of log on ground	All of log on ground
	Invaded by roots	No	No	Sapwood area	Throughout	Throughout
	Indirect measure	Cambium still fresh, died less than 1 year	Cambium decayed, knife blade penetrates a few millimeters	Knife blade penetrates less than 2 cm	Knife blade penetrates 2–5 cm	Knife blade penetrates all the way
Stumps	Indirect measure	Cambium still fresh, died less than 1 year	Cambium decayed, knife blade penetrates a few millimeters	Knife blade penetrates less than 2 cm	Knife blade penetrates 2–5 cm	Knife blade penetrates all the way

2.3. Calculation of Forest Biomass

Forest biomass includes the mass of living trees, shrubs, herbs, litter, and CWD. The species and DBH of all living trees in each plot were documented in each census to estimate the biomass, which was calculated using a regression model developed in a previous study in this region (Table 3) [35]. To reduce disturbance, based on a plot investigation, we selected five 2 m × 2 m shrub, and 1 m × 1 m nested herbal subplots outside the plot in each census to estimate the biomass of the shrubs, herbs, and litter. These subplots were not repeated each census, and new subplots were selected each time. The aboveground biomass of the shrubs, herbs, and litter was quantified by harvesting, and the belowground biomass of the shrubs and herbs was quantified by digging [19].

Table 3. The regression model of biomass and height in *P. armandi* and *Q. aliena* var. *acuteserrata* forests in the Huoditang Experimental Forest Farm in the Qinling Mountains (China).

Forest Types	Contents	Regression Equation	Correlation Coefficient	Reliability of 95% of the Estimated Accuracy
<i>Q. aliena</i> var. <i>acuteserrata</i>	Stem	$\ln W_S = 0.99253 \ln(D^2H) - 3.78818$	0.99763	94.24
	Bark	$\ln W_{BA} = 0.75632 \ln(D^2H) - 3.92450$	0.99708	95.37
	Branch	$\ln W_B = 3.49934 \ln D - 6.50726$	0.96524	84.27
	Leaf	$\ln W_L = 2.29344 \ln D - 4.88581$	0.97832	84.45
	Root	$\ln W_R = 2.76435 \ln D - 4.20817$	0.99106	89.15
	Height	$\frac{1}{H} = \frac{8.01921}{D^{2.59222}} + 0.05263$	0.78814	95.60
<i>P. armandi</i>	Stem	$\ln W_S = 1.02363 \ln(D^2H) - 4.49970$	0.99802	97.09
	Bark	$\ln W_{BA} = 0.88417 \ln(D^2H) - 5.38472$	0.99698	96.73
	Branch	$\ln W_B = 2.57551 \ln D - 4.08452$	0.98656	90.60
	Leaf	$\ln W_L = 2.75687 \ln D - 5.75891$	0.98004	81.56
	Root	$\ln W_R = 0.97120 \ln(D^2H) - 5.26301$	0.97927	92.13
	Height	$\frac{1}{H} = \frac{1.34537}{D^{1.70800}} + 0.07143$	0.88076	98.52

D = DBH (cm); H = Height of tree (m); W_S = Dry weight of stem (kg); W_{BA} = Dry weight of bark (kg); W_B = Dry weight of branch (kg); W_L = Dry weight of leaf (kg); W_R = Dry weight of roots (kg).

Tree species, compositions, decomposition stages, length, DBH, and the basal and distal ends of diameter for each piece of CWD in each plot were all reinvestigated each census. The shifts in CWD between CWD compositions, diameters, and decay classes were also documented each census, which would be expected to occur over the course of twenty years (i.e., snags became logs, CWD moved from decay class 2 to decay class 3, etc.). Prior to calculating CWD mass, the CWD density and volume were calculated. These CWD were allowed to decay naturally, and according to the investigation of the CWD in each plot from each census, CWD samples were all collected in August 2016. A total of 100 CWD samples were collected to calculate the density of the CWD (D_{sample} , Table 4), which included two species at five decay classes and four diameter classes (10–20 cm, 20–30 cm, 30–40 cm, and >40 cm). It should be noted that one assumption of this study was that density was constant throughout a log, snag, or stump. When the dead woods were lower decay classes, the stem and bark of the CWD was cut into disks approximately 2 cm thick using a handsaw. For more advanced decay classes, the CWD samples were simply transferred onto aluminum plates. The samples were immediately sealed in plastic bags, transported to the laboratory, and the sample volume (V_{sample}) was determined gravimetrically by water displacement. The CWD samples were then dried to a constant weight at 70 °C. The D_{sample} was estimated as the ratio of dry mass to V_{sample} .

We regarded the volume of each piece of log, snag, or stump as V_{CWD} . As each log or stump can be considered as a cylinder, we consequently used Smalian's formula to produce a volume estimate through the length and cross-sectional areas at the basal and distal ends of the cylinder [36]:

$$V_{\text{CWD}} = L \left[\frac{\pi(D_1/2)^2 + \pi(D_2/2)^2}{2} \right] \quad (1)$$

where V_{CWD} (m^3) is the volume of the piece of log or stump; L (m) is the length of the piece of log or stump; D_1 (m) is the diameter at the basal end; and D_2 (m) is the diameter at the distal end. It should be noted that this formula tends to slightly overestimate volume due to the natural taper of the material [37]. For snags, we inserted the height and diameter of each relevant sample into a species-specific wood volume equation (Table 3) [35].

Table 4. Mean densities of CWD at five decay classes and four diameter classes in *Q. aliena* var. *acuteserrata* and *P. armandi* ($g \cdot cm^{-3}$).

Tree Species	Decay Classes	Diameter Classes			
		10–20 cm	20–30 cm	30–40 cm	>40 cm
<i>Q. aliena</i> var. <i>acuteserrata</i>	1	0.64 (0.04, $n = 3$)	0.66 (0.03, $n = 3$)	0.67 (0.03, $n = 3$)	0.70 (0.05, $n = 2$)
	2	0.55 (0.03, $n = 3$)	0.56 (0.03, $n = 3$)	0.58 (0.04, $n = 3$)	0.60 (0.04, $n = 3$)
	3	0.41 (0.04, $n = 2$)	0.42 (0.04, $n = 3$)	0.44 (0.03, $n = 3$)	0.45 (0.03, $n = 2$)
	4	0.30 (0.02, $n = 3$)	0.33 (0.03, $n = 3$)	0.35 (0.03, $n = 3$)	0.32 (0.03, $n = 2$)
	5	0.20 (0.02, $n = 2$)	0.23 (0.02, $n = 2$)	0.22 (0.02, $n = 2$)	0.20 (0.02, $n = 2$)
<i>P. armandi</i>	1	0.35 (0.03, $n = 3$)	0.36 (0.03, $n = 3$)	0.37 (0.03, $n = 3$)	0.38 (0.04, $n = 2$)
	2	0.30 (0.02, $n = 2$)	0.30 (0.03, $n = 2$)	0.32 (0.03, $n = 2$)	0.32 (0.03, $n = 3$)
	3	0.25 (0.02, $n = 3$)	0.26 (0.02, $n = 2$)	0.26 (0.02, $n = 3$)	0.27 (0.02, $n = 2$)
	4	0.21 (0.02, $n = 2$)	0.22 (0.02, $n = 3$)	0.23 (0.02, $n = 2$)	0.23 (0.02, $n = 2$)
	5	0.17 (0.01, $n = 3$)	0.19 (0.02, $n = 2$)	0.17 (0.02, $n = 2$)	0.17 (0.01, $n = 2$)

Note: The standard errors of the mean are provided in parentheses, and n = the numbers of CWD samples.

Finally, the CWD mass ($Mg \cdot ha^{-1}$) for each plot in each census was calculated as the product of D_{sample} and V_{CWD} , correspondingly, e.g., we assumed that there were 5 pieces of CWD at mixed forest 3# in 2006 (1 for *P. armandi* at 1 decay class and 20–30 cm, 2 for *Q. aliena* var. *acuteserrata* at 2 decay class and 10–20 cm, 1 for *P. armandi* at 3 decay class and 10–20 cm, and 1 for *Q. aliena* var. *acuteserrata* at 4 decay class and 20–30 cm); thus we can get each CWD density from Table 4.

2.4. Statistical Analyses

The effects of stand age, forest type, CWD composition, decay class, and diameter class on the CWD mass were tested, and the interactions between these effect factors were also tested using two-way ANOVA with SAS 8.0 software (SAS inc. Carey, NC, USA). If there were significant effects, Duncan's t -test was used for mean separation. In our study, ΔCWD is the average annual increment of CWD mass, which conveys the dynamics of CWD mass over twenty years. ΔCWD implies the net change from one CWD census to the next, and would therefore include CWD input and decomposition.

Additionally, to identify the effects of the factors (forest biomass, stand age, forest type, altitude, aspect, slope, stand density, annual average temperature, and precipitation) on the CWD compositions, decay classes, and diameter classes in the different plots, redundancy analysis (RDA) was performed and visualized by the vegan R package 3.3.3. We transformed the aspect data to four directional categories, as follows: North (315° – 45°), East (45° – 135°), South (135° – 225°), West (225° – 315°). The transformed aspect data was applied to perform the RDA. The functions of `envfit` (999 random permutations) were used to test the significant correlations among the effect factors and CWD compositions, decay and diameter classes. For all analyses, the variability of the mean value was the standard error of the mean (SEM), and statistical significance was determined at $p = 0.05$.

3. Results

3.1. Dynamics of the Forest Biomass

There was a significant difference in forest biomass across the three forest types and nine censuses ($p = 0.0108$), ranging from (mean \pm SEM) $122.82 \pm 7.68 Mg \cdot ha^{-1}$ (*P. armandi* forest in 1996) to $336.69 \pm 12.88 Mg \cdot ha^{-1}$ (*Q. aliena* var. *acuteserrata* forest in 2016, Figure 3). The average

forest biomass in the *Q. aliena* var. *acuteserrata* forest ($259.24 \pm 9.75 \text{ Mg}\cdot\text{ha}^{-1}$) was significantly higher than that in the *P. armandi* ($174.38 \pm 8.64 \text{ Mg}\cdot\text{ha}^{-1}$) and mixed forests ($188.50 \pm 7.88 \text{ Mg}\cdot\text{ha}^{-1}$) from 1996–2016 ($p = 0.0186$). Over time, the forest biomass increased linearly from 1996 to 2016 in all forest types. The average annual biomass increment in the *Q. aliena* var. *acuteserrata* forest ($7.82 \pm 1.03 \text{ Mg}\cdot\text{ha}^{-1}\cdot\text{year}^{-1}$) was significantly higher than that in the *P. armandi* ($5.06 \pm 0.82 \text{ Mg}\cdot\text{ha}^{-1}\cdot\text{year}^{-1}$) and mixed forests ($5.15 \pm 0.91 \text{ Mg}\cdot\text{ha}^{-1}\cdot\text{year}^{-1}$, $p = 0.0215$). The forest biomass was dominated by live tree biomass, occupying greater than 88%; followed by CWD mass comprising of 6%–10%. In contrast, the understory biomass contribution to total forest biomass (1%–4%) was relatively small. The average understory biomass in the mixed forest ($5.24 \pm 0.75 \text{ Mg}\cdot\text{ha}^{-1}$) was slightly but insignificantly higher than that in the *Q. aliena* var. *acuteserrata* ($5.19 \pm 1.04 \text{ Mg}\cdot\text{ha}^{-1}$) and *P. armandi* forests ($5.08 \pm 0.87 \text{ Mg}\cdot\text{ha}^{-1}$) from 1996–2016 ($p = 0.9312$). The average CWD mass in the *P. armandi* forest ($16.78 \pm 6.46 \text{ Mg}\cdot\text{ha}^{-1}$) was significantly higher than that in the *Q. aliena* var. *acuteserrata* ($14.50 \pm 5.80 \text{ Mg}\cdot\text{ha}^{-1}$) and mixed forests ($12.20 \pm 4.25 \text{ Mg}\cdot\text{ha}^{-1}$) from 1996–2016 ($p = 0.0188$). Over time, the CWD mass also increased linearly from 1996–2016 in all forest types. The effect of forest type on the ΔCWD reached a highly significant level ($p < 0.0001$), and the ΔCWD in the *P. armandi* forest ($1.02 \pm 0.31 \text{ Mg}\cdot\text{ha}^{-1}\cdot\text{year}^{-1}$) was significantly higher than that in the *Q. aliena* var. *acuteserrata* ($0.84 \pm 0.24 \text{ Mg}\cdot\text{ha}^{-1}\cdot\text{year}^{-1}$) and mixed forests ($0.62 \pm 0.21 \text{ Mg}\cdot\text{ha}^{-1}\cdot\text{year}^{-1}$).

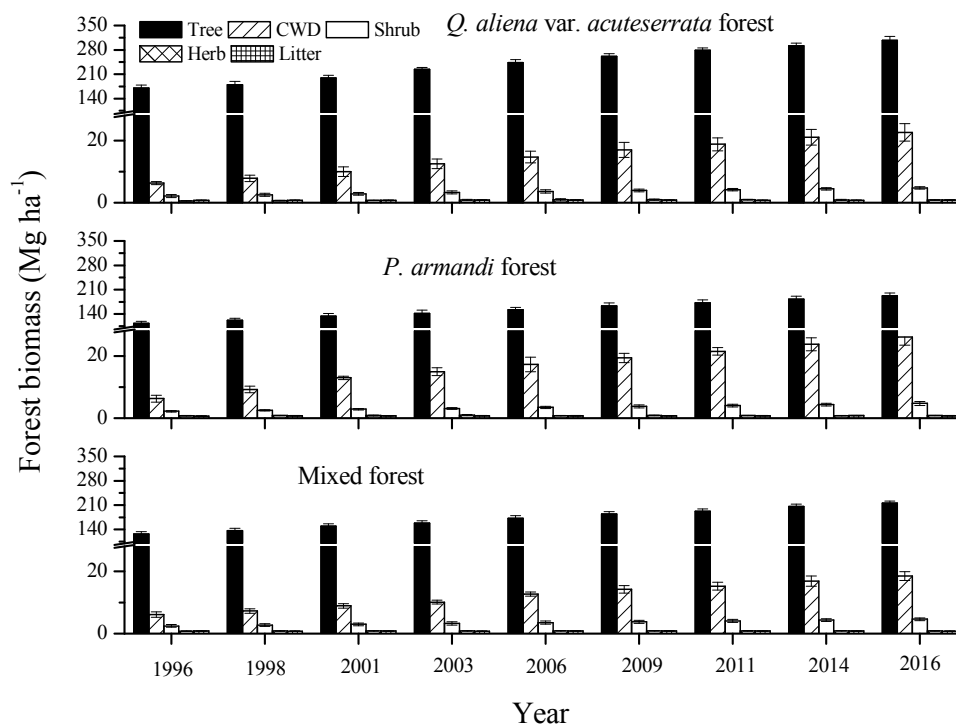


Figure 3. Forest biomass (the living trees, shrubs, herbs, litter and CWD) at the nine tree censuses during 1996–2016 for the three forest types in the Huoditang Experimental Forest Farm in the Qinling Mountains (China). The error bars represent the standard error of the mean, and are based on the plot as the experimental unit ($n = 6$).

3.2. Mass Characteristics of Coarse Woody Debris (CWD)

There was no significant difference in CWD mass among decay class, diameter class and composition ($p > 0.05$). The logs were the most common CWD component in the *Q. aliena* var. *acuteserrata* forest, followed by snags (Figure 4). However, logs and snags occupied about the same proportion of mass in the *P. armandi* and mixed forests. Over time, the masses of the logs, snags, and stumps all increased significantly from 1996–2016 in all forest types ($p = 0.0214$). In the *Q. aliena* var. *acuteserrata* forest ($0.59 \pm 0.11 \text{ Mg}\cdot\text{ha}^{-1}\cdot\text{year}^{-1}$) and *P. armandi* forest ($0.50 \pm 0.09 \text{ Mg}\cdot\text{ha}^{-1}\cdot\text{year}^{-1}$),

the average annual mass increment of logs was significantly higher ($p = 0.0102$) than the other CWD compositions. Meanwhile in the mixed forest, the mass increment of snags ($0.33 \pm 0.05 \text{ Mg}\cdot\text{ha}^{-1}\cdot\text{year}^{-1}$) was significantly higher ($p = 0.0312$). For all forest types, the mass increment of stumps was the lowest ($p = 0.0121$).

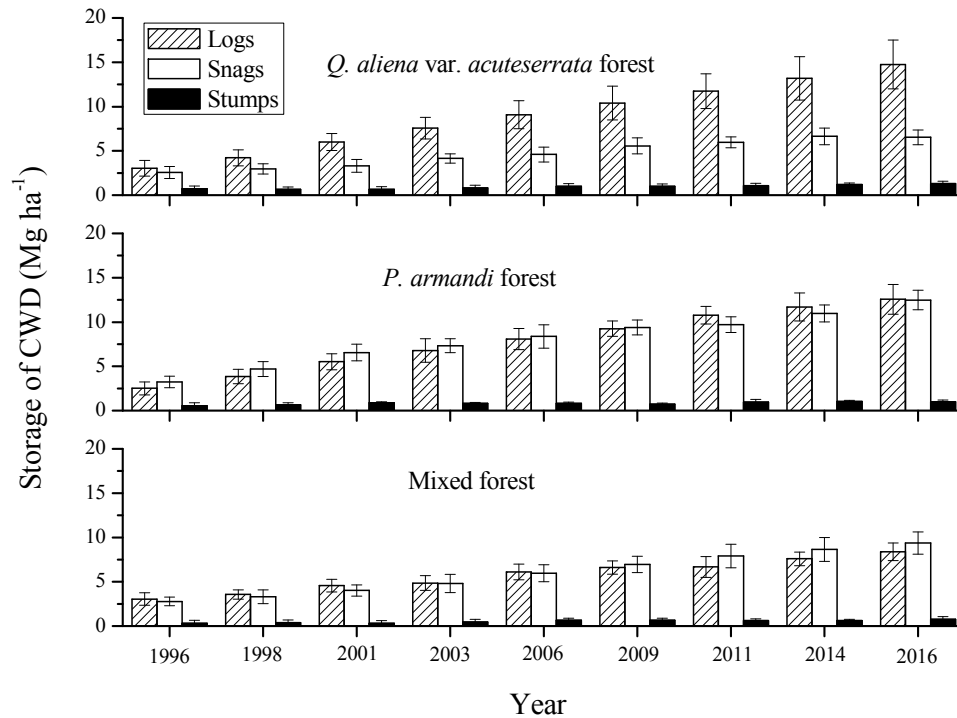


Figure 4. Mass of CWD compositions (logs, snags, and stumps) at the nine tree censuses during 1996–2016 for the three forest types in the Huoditang Experimental Forest Farm in the Qinling Mountains (China). The error bars represent the standard error of the mean, and are based on the plot as the experimental unit ($n = 6$).

In terms of CWD diameter, only the *P. armandi* forest had representation in the largest diameter class (>40 cm, Figure 5). The *Q. aliena* var. *acuteserrata* forest had the highest average CWD mass in the 20–30 cm class ($5.57 \pm 1.89 \text{ Mg}\cdot\text{ha}^{-1}$, $p = 0.0254$); *P. armandi* forest in the 10–20 cm ($6.76 \pm 2.18 \text{ Mg}\cdot\text{ha}^{-1}$) and 20–30 cm ($6.24 \pm 2.01 \text{ Mg}\cdot\text{ha}^{-1}$) classes ($p = 0.0311$); and mixed forests ($7.19 \pm 2.09 \text{ Mg}\cdot\text{ha}^{-1}$) in the smallest class (10–20 cm, $p = 0.0218$). Over time, the CWD masses of the different diameter classes all increased significantly from 1996–2016 in all forest types ($p = 0.0184$). The ΔCWD was significantly higher in the 10–20 cm class in the *P. armandi* ($0.37 \pm 0.05 \text{ Mg}\cdot\text{ha}^{-1}\cdot\text{year}^{-1}$) and mixed forests ($0.37 \pm 0.04 \text{ Mg}\cdot\text{ha}^{-1}\cdot\text{year}^{-1}$) ($p = 0.0268$), while it was significantly lower in the 30–40 cm class in the mixed forest ($0.05 \pm 0.008 \text{ Mg}\cdot\text{ha}^{-1}\cdot\text{year}^{-1}$) ($p = 0.0281$), except for the >40 cm class in the *P. armandi* forest ($0.03 \pm 0.006 \text{ Mg}\cdot\text{ha}^{-1}\cdot\text{year}^{-1}$).

The shifts in CWD mass between decay classes were different at the nine tree censuses during 1996–2016 for the three forest types; most of the shifts moved to decay class 1, and few to decay class 5 (Table 5). The *Q. aliena* var. *acuteserrata* forest had the highest average CWD mass in decay classes 1, 2 and 3 ($p = 0.0252$, Figure 6), and there was no significant difference among decay classes 1, 2 and 3 ($p = 0.1231$). *P. armandi* ($7.64 \pm 2.42 \text{ Mg}\cdot\text{ha}^{-1}$) and mixed forests ($4.55 \pm 2.12 \text{ Mg}\cdot\text{ha}^{-1}$) all had the highest average CWD mass in decay class 1 ($p = 0.0315$). All of the forest types had the lowest average CWD mass in decay class 5 ($p = 0.0151$). Over time, the CWD masses of the different decay classes all increased significantly from 1996–2016 in all forest types ($p = 0.0288$). In the *Q. aliena* var. *acuteserrata* forest, the ΔCWD was significantly the highest for decay class 1 ($0.21 \pm 0.06 \text{ Mg}\cdot\text{ha}^{-1}\cdot\text{year}^{-1}$) and decay class 2 ($0.20 \pm 0.04 \text{ Mg}\cdot\text{ha}^{-1}\cdot\text{year}^{-1}$, $p = 0.0294$), while in the *P. armandi*

($0.45 \pm 0.11 \text{ Mg}\cdot\text{ha}^{-1}\cdot\text{year}^{-1}$) and mixed forests ($0.33 \pm 0.08 \text{ Mg}\cdot\text{ha}^{-1}\cdot\text{year}^{-1}$), it was significantly the highest for decay class 1 ($p = 0.0213$). In all forest types, that was significantly the lowest for decay class 5 ($p = 0.0152$).

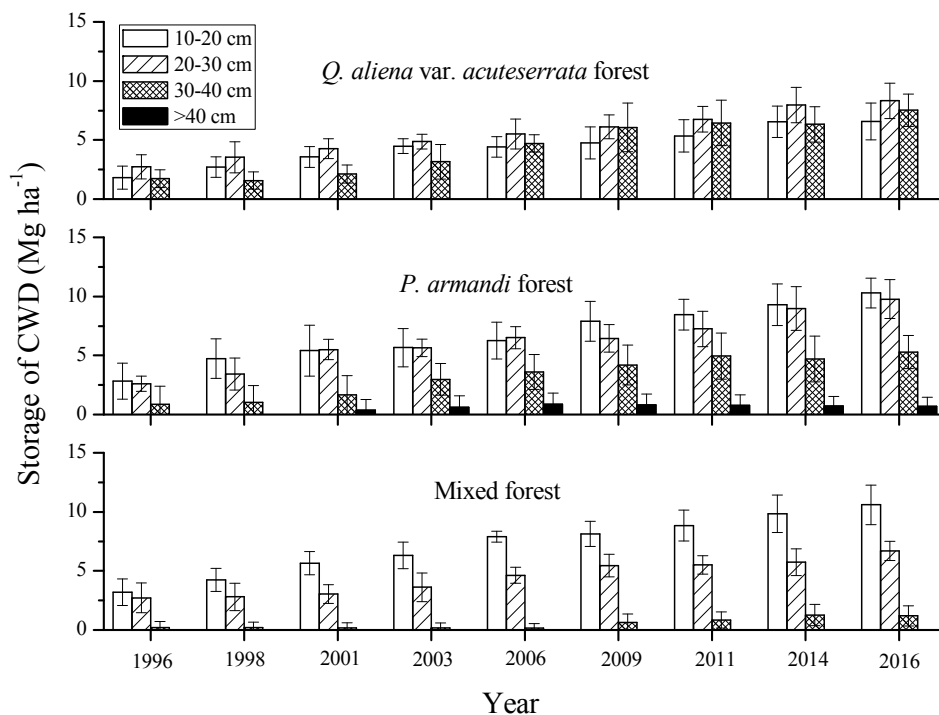


Figure 5. Mass of CWD diameter classes at the nine tree censuses during 1996–2016 for the three forest types in the Huoditang Experimental Forest Farm in the Qinling Mountains (China). The error bars represent the standard error of the mean, and are based on the plot as the experimental unit ($n = 6$).

Table 5. The shifts in CWD mass ($\text{Mg}\cdot\text{ha}^{-1}$) between decay classes at the nine tree censuses during 1996–2016 for the three forest types in the Huoditang Experimental Forest Farm in the Qinling Mountains (China).

Forest Types	Shifts between Decay Classes	Year							
		1998	2001	2003	2006	2009	2011	2014	2016
<i>Q. aliena</i> var. <i>acuteserrata</i>	0–1	1.57 (0.52)	1.75 (1.34)	0.42 (0.66)	0.53 (0.83)	0.84 (1.15)	0.19 (0.47)	0.33 (0.80)	0.46 (0.70)
	1–2	0.39 (0.60)	0.66 (0.84)	1.53 (1.03)	0.40 (0.98)	1.25 (0.92)	0	0.60 (0.75)	0.66 (0.98)
	2–3	0	0.23 (0.57)	0.74 (0.60)	1.10 (1.08)	0.51 (0.90)	0.96 (1.17)	1.10 (0.91)	0
	3–4	0	0	0.45 (0.50)	0.68 (0.77)	0.37 (0.57)	1.11 (0.58)	0.37 (0.61)	0.99 (0.60)
	4–5	0	0	0	0.43 (0.69)	0.19 (0.34)	0.76 (0.84)	0.73 (0.81)	0.42 (0.60)
<i>P. armandi</i>	0–1	3.11 (0.20)	1.22 (0.67)	0.81 (0.90)	1.38 (1.05)	0.66 (0.77)	0.98 (1.69)	0.86 (1.10)	1.12 (0.57)
	1–2	0	1.97 (0.83)	1.01 (0.80)	0.21 (0.51)	1.10 (1.01)	0.73 (1.19)	1.34 (0.81)	0.42 (0.66)
	2–3	0	0.67 (1.08)	0.78 (0.87)	0.80 (0.70)	0.47 (1.14)	0.69 (0.80)	0.17 (0.40)	0.66 (0.72)
	3–4	0	0	0	0.28 (0.68)	0.30 (0.74)	0.25 (0.62)	0.27 (0.50)	0.26 (0.63)
	4–5	0	0	0	0	0	0	0.30 (0.73)	0.33 (0.82)
Mixed forest	0–1	1.43 (0.21)	2.04 (0.77)	0.88 (0.68)	1.61 (0.74)	1.03 (0.77)	0	0.30 (0.52)	0.43 (0.64)
	1–2	0	0	0.63 (0.98)	1.25 (0.66)	0.65 (0.62)	0.92 (0.74)	0.64 (0.64)	0.81 (0.94)
	2–3	0	0	0	0	0.15 (0.36)	0.69 (0.76)	0.69 (0.64)	0.43 (0.60)
	3–4	0	0	0	0	0	0.15 (0.37)	0.48 (0.69)	0.61 (0.96)
	4–5	0	0	0	0	0	0	0.19 (0.46)	0

Note: The standard errors of the mean are provided in parentheses, and are based on the plot as the experimental unit ($n = 6$).

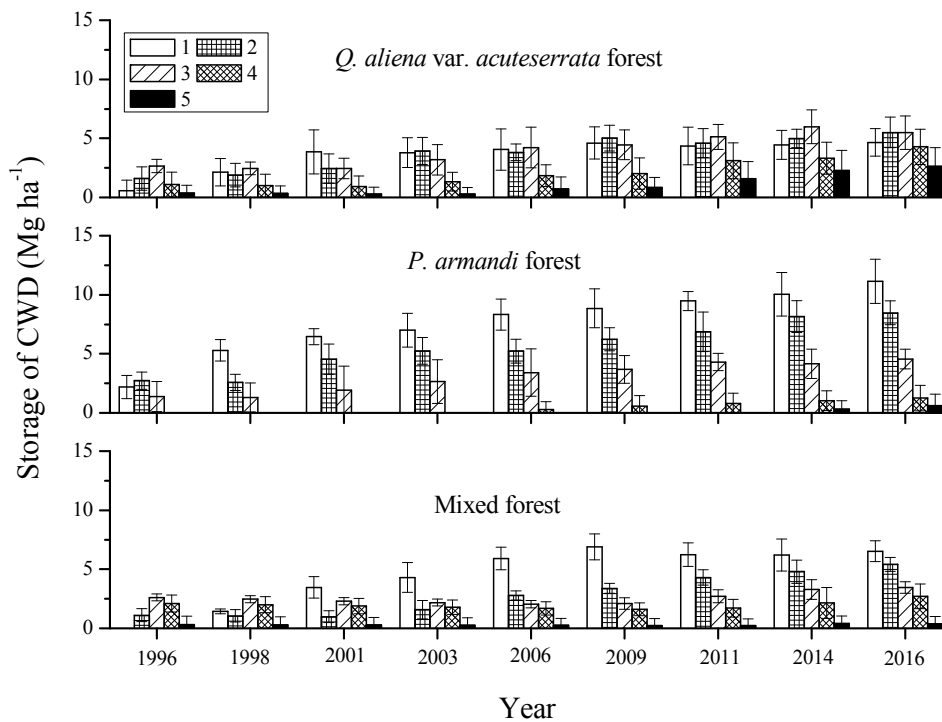


Figure 6. Mass of CWD decay classes at the nine tree censuses during 1996–2016 for the three forest types in the Huoditang Experimental Forest Farm in the Qinling Mountains (China). The error bars represent the standard error of the mean, and are based on the plot as the experimental unit ($n = 6$).

3.3. Redundancy Analysis (RDA)

Four different Redundancy Analysis (RDA) analyses were performed. In the first RDA analyses, effect factors and plot parameters were plotted with no distinction among the CWD compositions, decay classes, and diameter classes (Figure 7). The first axis (RDA1) accounted for 83% of observed variation and the second axis (RDA2) for 4%. Except for altitude ($p = 0.6589$), other factors were all significantly correlated with CWD mass ($p < 0.05$), and forest type exhibited the strongest correlation ($r^2 = 0.8964$). In the second RDA analyses, effect factors and plot parameters (explanatory variables) and CWD mass in compositions (response variables) were plotted (Figure 8). The first axis (RDA1) accounted for 72% of the observed variation and the second axis (RDA2) for 13%. Except for altitude ($p = 0.4652$), aspect ($p = 0.2063$), and slope ($p = 0.1325$), other factors were all significantly correlated with CWD compositions ($p < 0.05$), and stand age exhibited the strongest correlation ($r^2 = 0.8114$). In the third RDA analyses, effect factors and plot parameters (explanatory variables) and CWD mass in diameter classes (response variables) were plotted (Figure 9). The first axis (RDA1) accounted for 51% of observed variation and the second axis (RDA2) for 24%. Except for altitude ($p = 0.2365$), and slope ($p = 0.0895$), other factors were all significantly correlated with CWD diameter classes ($p < 0.05$), and stand age exhibited the strongest correlation ($r^2 = 0.8254$). In the fourth RDA analyses, effect factors and plot parameters (explanatory variables) and CWD mass in decay classes (response variables) were plotted (Figure 10). The first axis (RDA1) accounted for 57% of observed variation and the second axis (RDA2) for 12%. Except for altitude ($p = 0.6425$), aspect ($p = 0.1867$), and slope ($p = 0.0811$), other factors were all significantly correlated with CWD decay classes ($p < 0.05$), and stand age exhibited the strongest correlation ($r^2 = 0.7865$).

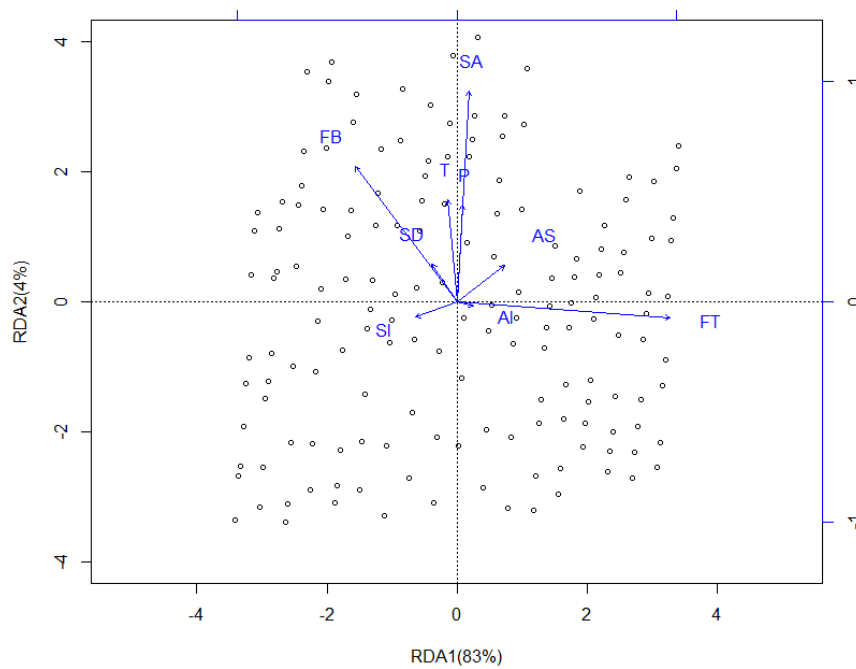


Figure 7. Redundancy Analysis (RDA) showing the relationships between the CWD mass and effect factors in the different samples on the Huoditang Experimental Forest Farm in the Qinling Mountains (China). Arrows indicate effect factors: FT = Forest type; FB = Forest biomass; AS = Aspect; Al = Altitude; SA = Stand age; Sl = Slope; SD = Stand density; T = Annual average temperature; P = Annual average precipitation.

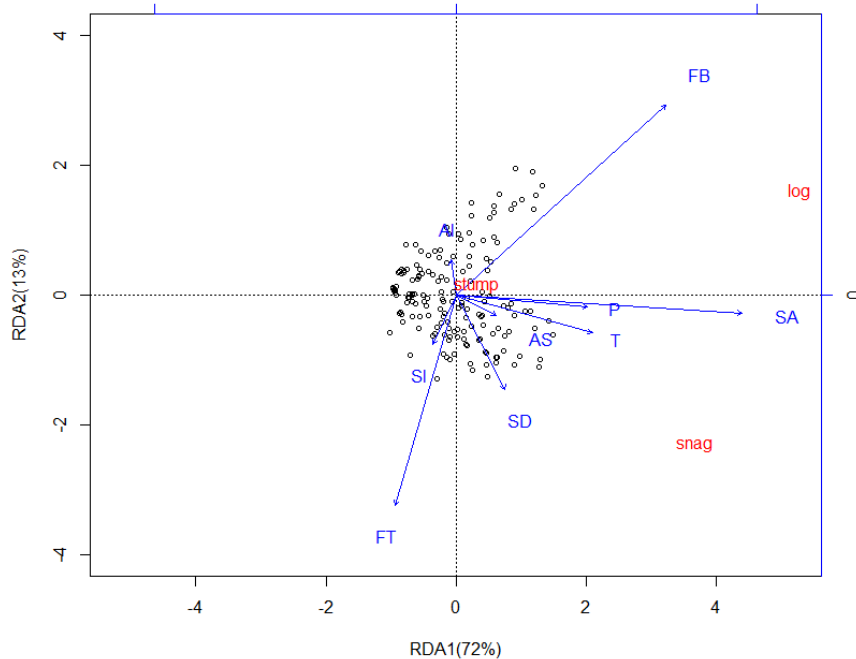


Figure 8. Redundancy Analysis (RDA) showing the relationships between the CWD compositions (logs, snags, and stumps) and effect factors in the different samples on the Huoditang Experimental Forest Farm in the Qinling Mountains (China). Arrows indicate effect factors: FT = Forest type; FB = Forest biomass; AS = Aspect; Al = Altitude; SA = Stand age; Sl = Slope; SD = Stand density; T = Annual average temperature; P = Annual average precipitation. CWD composition names in red indicate the composition's vector endpoints.

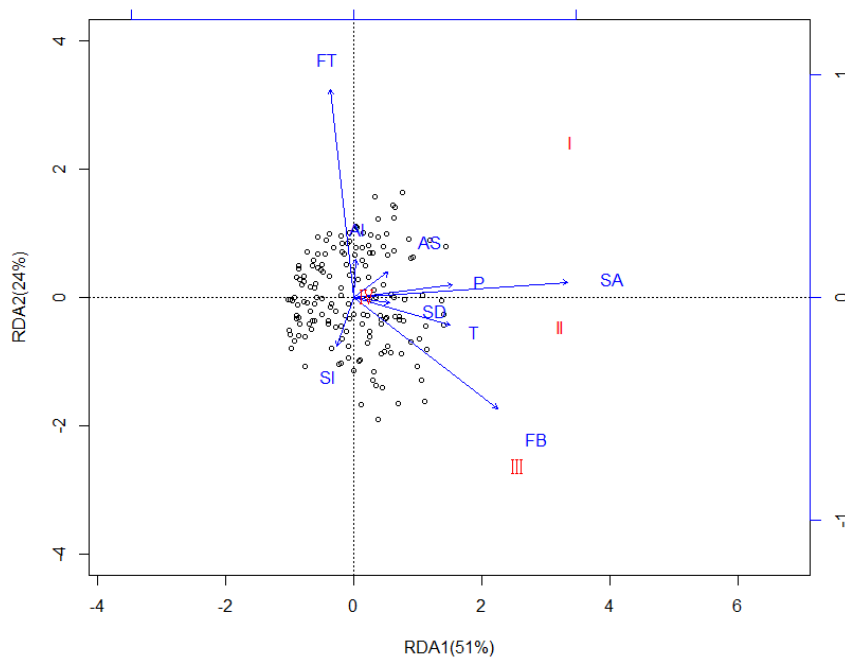


Figure 9. Redundancy Analysis (RDA) showing the relationships between the CWD diameter classes and effect factors in the different samples on the Huoditang Experimental Forest Farm in the Qinling Mountains (China). Arrows indicate effect factors: FT = Forest type; FB = Forest biomass; AS = Aspect; AI = Altitude; SA = Stand age; SI = Slope; SD = Stand density; T = Annual average temperature; P = Annual average precipitation. I: 10–20 cm, II: 20–30 cm, III: 30–40 cm, and IV: >40 cm. CWD diameter class names in red indicate the diameter class’s vector endpoints.

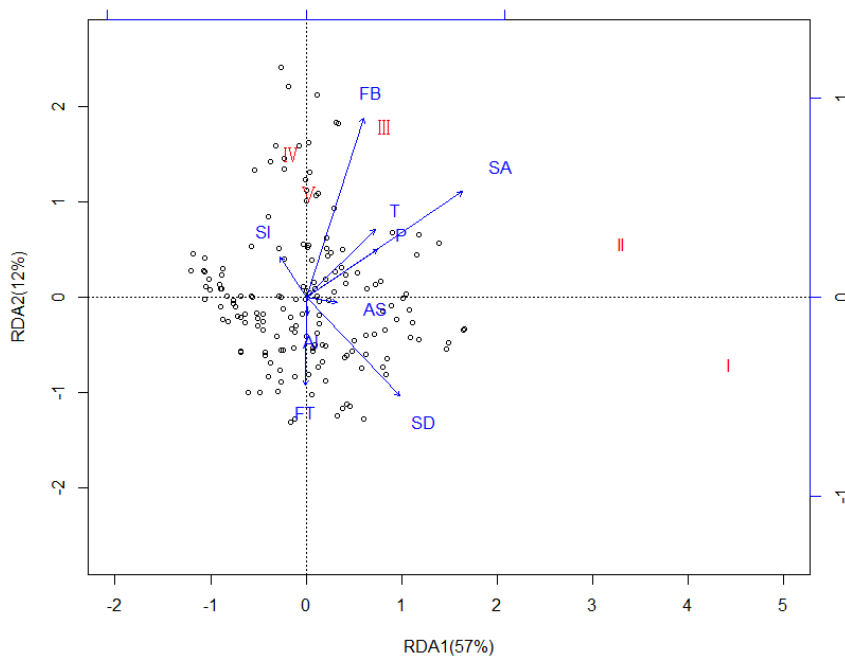


Figure 10. Redundancy Analysis (RDA) showing the relationships between the CWD decay classes and effect factors in the different samples on the Huoditang Experimental Forest Farm in the Qinling Mountains (China). Arrows indicate effect factors: FT = Forest type; FB = Forest biomass; AS = Aspect; AI = Altitude; SA = Stand age; SI = Slope; SD = Stand density; T = Annual average temperature; P = Annual average precipitation. CWD decay class names in red indicate the decay stage’s vector endpoints. The numbers I–V represent different decomposition stages where I represents the initial stages and V represents the final stage.

4. Discussion

The average forest biomass of the *Q. aliena* var. *acuteserrata* forest was the highest among the three forest types (Figure 3). The higher biomass stock was due to a higher mean annual accumulation rate, which may be caused by the higher leaf area index (5.21 in *Q. aliena* var. *acuteserrata* forest, 4.25 in mixed forest and 3.86 in *P. armandi* forest) and the larger leaf production efficiency ($0.82 \text{ Mg}\cdot\text{ha}^{-1}\cdot\text{year}^{-1}$ in *P. armandi* and $3.35 \text{ Mg}\cdot\text{ha}^{-1}\cdot\text{year}^{-1}$ in *Q. aliena* var. *acuteserrata*) [35]. Although the understory biomass contribution to total forest biomass was small (1%–4%), the understory has previously been shown to be an important component of the forest ecosystem, and plays an important role in maintaining the carbon balance between forest ecosystem and atmosphere [38,39]. The understory biomass was different in the three forest types (Figure 3), which may have been due to environmental heterogeneity (gap and sunflecks) and differences in biological traits (morphology, structure and function, etc.) of the understory species in these forests [39,40].

The CWD mass made up the second largest category of biomass after live tree biomass (Figure 3). If CWD was not included, previous studies have estimated global detritus could be underestimated by $2\text{--}16 \times 10^{13} \text{ kg}$ where the relative error associated with this value is 2%–10% [41].

The global range in the proportions of CWD mass to forest biomass varies from 10%–40% [42–45]. However, the datum we observed was 6%–10%, which was slightly lower than the lower limit of the global records. In our study, there was a strong correlation between CWD mass and forest biomass. This result has been reported in several studies [26,45,46]; however, the dependence of CWD mass on forest biomass differs between forest types [19]. Moreover, the diameter classes, decomposition stages, species composition, and the proportion of CWD mass to forest biomass may affect the dependence of CWD mass on forest biomass [45]. Aakala et al. considered that the influence of the disturbance history of the stands was also a crucial factor for the dependence of CWD mass on forest biomass [47].

In forest ecosystems, different CWD compositions (i.e., logs, snags, and stumps) can be an indicator of origin and legacy of CWD [27]. In addition, it can be used to reflect forest management and stand development history. Yan et al. concluded that a higher proportion of CWD (due to stumps at a given site) may suggest extensive anthropogenic disturbances in the past such as clear-cutting or selective logging [27]. In the 1960s and 1970s, intensive selective logging occurred in this area. Unexpectedly, the stumps did not appear to be an apparent symbol for past selective logging as we failed to record a high level of mass from the stumps in the three forests (Figure 4). Perhaps after four or five decades of decomposition, most of the stumps left either constituted an incomplete and loose structure, giving rise to failure to assess valid volumes, or disappeared.

Our results showed that logs were a principal CWD input source over a period of 20 years (Figure 4), which was consistent with other studies described in References [13,48,49]. We considered that the substantial mass in logs in the study area primarily resulted from the local pulses (in summer of 2015) in mortality, driven by a combination of strong winds, and steep topography. However, the snags in *P. armandi* and mixed forests occupied about the same proportion of mass to logs (Figure 4). The resistance of physiology and biochemistry in the phloem of trees in *P. armandi* and mixed forests was decreased, and the reduction of nutrition was accelerated by the attacking of insects and diseases, which were mainly caused by a recorded infestation of *D. armandi*.

According to our long-term monitoring, we could obtain the precise values for the shifts in CWD mass between decay classes (Table 5), which was informative for decomposition dynamics. The shifts were different in the three forest types; this may be caused by the different decay rates between *P. armandi* and *Q. aliena* var. *acuteserrata* CWD [19]. In addition, due to the lower decay rate in *P. armandi* CWD, more CWD was retained at lower decay classes, and less CWD mass was lost, which may be a reason for higher CWD mass in the *P. armandi* forest.

CWD in the three forests had significantly different decomposition stages (Figure 6) and diameter classes (Figure 5). The latest wind throw events could be propitious to shed light on the origin of the high mass in the early stage of the decay class, especially in steep topography. Our study showed that the CWD mass in advanced decomposition classes increased over 20 years (Figure 6), which was

consistent with Carmona et al. [30] and Motta et al. [50]. Moreover, CWD mass in large diameter classes also increased during 1996–2016 (Figure 5), which was also reported by others in References [30,48]. Noticeably, the occurrence of large living trees is an essential prerequisite for creating large size CWD, but these were scarce in the three forests. The removal of large logs after intensive selective logging may partially explain why CWD with larger sizes (>40 cm) was scarce in our study area.

Our study revealed that the forest type exhibited the strongest correlation with CWD mass (Figure 7). The average CWD mass in the *P. armandi* forest was the highest, reaching $16.78 \pm 6.46 \text{ Mg}\cdot\text{ha}^{-1}$. The datum was less than the lower limit of the global range in the CWD mass of natural coniferous forests which varied from $30 \text{ Mg}\cdot\text{ha}^{-1}$ to $200 \text{ Mg}\cdot\text{ha}^{-1}$ [41]. However, Li et al. reported an equivalent amount ($15.848 \text{ Mg}\cdot\text{ha}^{-1}$) in CWD from the *Abies fargesii* forest near our study site [51]; even He et al. ($7.706 \text{ Mg}\cdot\text{ha}^{-1}$) [52] and Yuan et al. ($12.56 \text{ Mg}\cdot\text{ha}^{-1}$) [53] showed a lower value in an adjacent natural forest of *P. tabulaeformis*. The global range in the CWD mass of broad-leaved forests varied from $8 \text{ Mg}\cdot\text{ha}^{-1}$ to $50 \text{ Mg}\cdot\text{ha}^{-1}$ [54]. The data we observed in the *Q. aliena* var. *acuteserrata* forest was the lower limit of the global records, and was lower than that measured in the monsoon evergreen broad-leaved forest of Dinghushan ($17.41 \text{ Mg}\cdot\text{ha}^{-1}$ – $38.54 \text{ Mg}\cdot\text{ha}^{-1}$) [25], but was higher than that examined in the 76-year old *Castanopsis eyrei* forest in the Wuyi Mountains ($7.349 \text{ Mg}\cdot\text{ha}^{-1}$) [55].

The *P. armandi* forest was vulnerable to pests and fungi, especially by *D. armandi* infestation, which may be mainly due to the volatiles of *P. armandi* [56]. The live *P. armandi* was attacked by *D. armandi*, and then died to become snags. This explanation might reveal why the CWD mass in the *P. armandi* forest was significantly higher than the other types. Greater ecosystem stability, resistance to disturbance ability and vigor were likely due to greater biodiversity; the mixed forest was less vulnerable to diseases and pests, which may explain the lower CWD mass in the mixed forest. The accumulation in CWD is expected to be dynamically mediated by various CWD production and decomposition-controlling factors [57]. Overall, the comparatively low CWD mass could be explained by low rates of ΔCWD . The ΔCWD in the three forests were all lower than that measured in a monsoon evergreen broad-leaved forest of Dinghushan ($1.32 \text{ Mg}\cdot\text{ha}^{-1}\cdot\text{year}^{-1}$) [25] and in an *Abies fargesii* forest close to our study site ($1.88 \text{ Mg}\cdot\text{ha}^{-1}\cdot\text{year}^{-1}$) [51].

Our results showed that aspect and slope were both significantly positively correlated with CWD mass (Figure 7). In general, most CWD in natural forests are derived from gradual accumulation after ecosystems suffer severe disturbances (e.g., wind throw) [13]. We considered that the substantial CWD in our study area may primarily be driven by a combination of strong winds and steep topography. This explanation was supported by the fact that over 50% of logs were usually observed on mountain ridges, windward slopes, and abrupt slopes. According to our investigation, we found that most snags were produced on the south-facing slopes, which was expected to be relative to its shade intolerance.

Stand density was another factor significantly correlated with CWD mass. On the one hand, higher stand density may produce more intense competition for resources in overcrowding habitats leading to higher mortality rates. On the other hand, higher stand density may also cause vegetation to be more susceptible to disturbances. Moreover, our study concluded that the stand age had a significant effect on CWD mass (Figure 7). Harmon et al. suggested that the CWD mass pattern paralleled the stand development to show a “U” shape pattern [13]. The decomposition of CWD was a slow and long-term process, and we assumed that the decay rate was a constant in all the forest developmental stages. Thus, we considered that the “U” shape pattern was also to be found in the tree mortality. The same “U” shape pattern was also observed by other studies described in References [27,58,59].

What should be noted is that the estimated annual average temperatures in these sample plots may be inaccurate. Although we assumed a standard lapse rate of $0.7 \text{ }^\circ\text{C}$ in this forest area, there were still error sources when estimating the annual average temperatures in these sample plots. In our study, the error sources for estimating the annual average temperature mainly included the standard lapse rate, aspect, and forest microclimate. Thus, the effects of the annual average temperature on the CWD compositions, decay classes, and diameter classes may have been undervalued.

Within a suitable temperature and moisture range for the growth of microorganisms, higher temperature and precipitation may accelerate the decomposition of CWD [60,61], which could therefore retain less CWD mass. However, drought and rainstorms may produce abundant CWD mass. Furthermore, a surge in CWD mass may also be suddenly created by serious windstorms. For instance, in 1986, a catastrophic tornado suddenly produced up to 1000 ha of logs in the Changbai Mountain [41]. In natural *Rhododendron simiarum* forests in the Tianbaoyan National Nature Reserve, with an increase in elevation, the CWD mass displayed an ever-increasing trend [62]. This suggested that higher elevations might form greater wind speeds and cause higher tree mortality. However, our study selected a narrow altitude range (1410–1983 m), and wind speed was not significantly different. Thus, our study considered that altitude was not significantly correlated with CWD mass in these forests. In addition, methodological difference between studies (e.g., minimum diameter chosen, whether they exclude or include standing dead trees, etc.) may result in differences in CWD mass estimations, thus making comparisons difficult. Additionally, plot size, or transect length may also influence whether the sampling adequately captured the full spatial variations in forest structure [37].

5. Conclusions

Overall, we believe that CWD distribution in the three forests was a result of comprehensive influences from the forest developmental stage caused by past selective logging, and natural and anthropogenic interferences. We conducted nine tree censuses between 1996 and 2016 to help us quantify CWD dynamics over a period of 20 years. The results showed that the long-term monitoring of the dynamics of forest biomass (including CWD) was beneficial to clarifying the role of CWD in carbon cycles of forest ecosystems. Meantime, the long-term monitoring can acquire the multiple effect factors on CWD mass, which was necessary to reveal the reasons for the accumulation of CWD. In forest ecosystems, characteristics of CWD can be expected to reflect forest stand features which was also evident in our study. Our study showed that CWD mass made up the second largest category of biomass after live tree biomass, and occupied 6–10%. Moreover, CWD mass in advanced decomposition classes and large diameter classes all increased during 1996–2016. Our study provided precise and detailed dynamics of CWD characteristics, and identified the effect factors on the CWD characteristics, which are indispensable for development of CWD reasonable strategies in future forest management.

Acknowledgments: We are grateful to the Qinling National Forest Ecosystem Research Station for providing some data and the experimental equipment. This research was funded by the project of “Technical management system for increasing the capacity of carbon sink and water regulation of mountain forests in the Qinling Mountains” (201004036) from the State Forestry Administration of China.

Author Contributions: S.Z. and J.Y. conceived and designed the experiments; J.Y., X.Z. and F.C. performed the experiments; J.Y., S.J., L.H. and J.L. analyzed results and wrote the manuscript text.

Conflicts of Interest: The authors declare no conflict of interest.

References

1. Montes, F.; Canellas, I. Modelling coarse woody debris dynamics in even-aged *Scots pine* forests. *For. Ecol. Manag.* **2006**, *221*, 220–232. [[CrossRef](#)]
2. Janisch, J.; Harmon, M. Successional changes in live and dead wood carbon stores: Implications for net ecosystem productivity. *Tree Physiol.* **2002**, *22*, 77–89. [[CrossRef](#)] [[PubMed](#)]
3. Zimmerman, J.K.; Waide, R.B. Nitrogen immobilization by decomposing woody debris and the recovery of tropical wet forest from hurricane damage. *Oikos* **1995**, *72*, 314–322. [[CrossRef](#)]
4. Wei, X.; Kimmins, J.P.; Peel, K.; Steen, O. Mass and nutrients in woody debris in harvested and wildfire-killed lodgepole pine forests in the central interior of British Columbia. *Can. J. For. Res.* **2011**, *27*, 148–155. [[CrossRef](#)]
5. Arthur, M.A.; Fahey, T.J. Mass and nutrient content of decaying boles in an Engelmann spruce-subalpine fir forest, Rocky Mountain National Park, Colorado. *Can. J. For. Res.* **1990**, *20*, 730–737. [[CrossRef](#)]

6. Chen, H.; Xu, Z.B. History, current situation and tendency of CWD ecological research. *Chin. J. Ecol.* **1991**, *10*, 45–50, (In Chinese, with English abstract).
7. Gough, C.M.; Vogel, C.S.; Kazanski, C.; Nagel, L.; Flower, C.E.; Curtis, P.S. Coarse woody debris and the carbon balance of a north temperate forest. *For. Ecol. Manag.* **2007**, *244*, 60–67. [[CrossRef](#)]
8. Woodall, C.W.; Liknes, G.C. Relationships between forest fine and coarse woody debris carbon stocks across latitudinal gradients in the United States as an indicator of climate change effects. *Ecol. Indic.* **2008**, *8*, 686–690. [[CrossRef](#)]
9. Harmon, M.E.; Franklin, J.F. Tree seedlings on logs in Picea-Tsuga forests of Oregon and Washington. *Ecology* **1989**, *70*, 48–59. [[CrossRef](#)]
10. Santiago, L.S. Use of coarse woody debris by the plant community of a Hawaiian montane cloud forest. *Biotropica* **2000**, *32*, 633–641. [[CrossRef](#)]
11. Mac Nally, R.; Parkinson, A.; Horrocks, G.; Conole, L.; Tzaros, C. Relationships between terrestrial vertebrate diversity, abundance and availability of coarse woody debris on south-eastern Australian floodplains. *Biol. Conserv.* **2001**, *99*, 191–205. [[CrossRef](#)]
12. Stevenson, S.K.; Jull, M.J.; Rogers, B.J. Abundance and attributes of wildlife trees and coarse woody debris at three silvicultural systems study areas in the Interior Cedar-Hemlock Zone, British Columbia. *For. Ecol. Manag.* **2006**, *233*, 176–191. [[CrossRef](#)]
13. Harmon, M.E.; Franklin, J.F.; Swanson, F.J.; Sollins, P.; Gregory, S.; Lattin, J.; Anderson, N.; Cline, S.; Aumen, N.; Sedell, J. Ecology of coarse woody debris in temperate ecosystems. *Adv. Ecol. Res.* **1986**, *15*, 133–302.
14. Magnússon, R.Í.; Tietema, A.; Cornelissen, J.H.C.; Hefting, M.M.; Kalbitz, K. Tamm review: Sequestration of carbon from coarse woody debris in forest soils. *For. Ecol. Manag.* **2016**, *377*, 1–15. [[CrossRef](#)]
15. Brovkin, V.; Bodegom, P.M.V.; Kleinen, T.; Wirth, C. Plant-driven variation in decomposition rates improves projections of global litter stock distribution. *Biogeosciences* **2012**, *9*, 565–576. [[CrossRef](#)]
16. Harmon, M.E.; Ferrell, W.K.; Franklin, J.F. Effects on carbon storage of conversion of old-growth forests to young forests. *Science* **1990**, *247*, 699–702. [[CrossRef](#)] [[PubMed](#)]
17. Bradford, J.; Weishampel, P.; Smith, M.L.; Kolka, R.; Birdsey, R.A.; Ollinger, S.V.; Ryan, M.G. Detrital carbon pools in temperate forests: Magnitude and potential for landscape-scale assessment. *Can. J. For. Res.* **2009**, *39*, 802–813. [[CrossRef](#)]
18. Russell, M.B.; Woodall, C.W.; Fraver, S.; D’Amato, A.W.; Domke, G.M.; Skog, K.E. Residence times and decay rates of downed woody debris biomass/carbon in eastern US forests. *Ecosystems* **2014**, *17*, 765–777. [[CrossRef](#)]
19. Yuan, J.; Hou, L.; Wei, X.; Shang, Z.C.; Cheng, F.; Zhang, S.X. Decay and nutrient dynamics of coarse woody debris in the Qinling Mountains, China. *PLoS ONE* **2017**, *12*, e0175203. [[CrossRef](#)] [[PubMed](#)]
20. Silva, L.F.S.G.; Castilho, C.V.D.; Cavalcante, C.D.O.; Pimentel, T.P.; Fearnside, P.M.; Barbosa, R.I. Production and stock of coarse woody debris across a hydro-edaphic gradient of oligotrophic forests in the northern Brazilian Amazon. *For. Ecol. Manag.* **2016**, *364*, 1–9. [[CrossRef](#)]
21. Sefidi, K.; Darabad, F.E.; Azaryan, M. Effect of topography on tree species composition and volume of coarse woody debris in an *Oriental beech* (*Fagus orientalis* Lipsky) old growth forests, northern Iran. *iForest* **2016**, *9*, e1–e8.
22. Palviainen, M.; Finér, L.; Laiho, R.; Shorohova, E.; Kapitsa, E.; Vanha-Majamaa, I. Carbon and nitrogen release from decomposing *Scots pine*, Norway spruce and silver birch stumps. *For. Ecol. Manag.* **2010**, *259*, 390–398.
23. Muller-Using, S.; Bartsch, N. Decay dynamic of coarse and fine woody debris of a beech (*Fagus sylvatica* L.) forest in Central Germany. *Eur. J. For. Res.* **2009**, *128*, 287–296. [[CrossRef](#)]
24. Sato, T.; Yagihashi, T.; Niiyama, K.; Kassim, A.R.; Ripin, A. Coarse woody debris stocks and inputs in a primary hill dipterocarp forest, Peninsular Malaysia. *J. Trop. For. Sci.* **2016**, *28*, 382–391.
25. Yang, F.F.; Li, Y.L.; Zhou, G.Y.; Wenigmann, K.O.; Zhang, D.Q.; Wenigmann, M.; Liu, S.Z.; Zhang, Q.M. Dynamics of coarse woody debris and decomposition rates in an old-growth forest in lower tropical China. *For. Ecol. Manag.* **2010**, *259*, 1666–1672. [[CrossRef](#)]
26. Siitonen, J.; Martikainen, P.; Punttila, P.; Rauh, J. Coarse woody debris and stand characteristics in mature managed and old-growth boreal mesic forests in southern Finland. *For. Ecol. Manag.* **2000**, *128*, 211–225.

27. Yan, E.R.; Wang, X.H.; Huang, J.J.; Zeng, F.R.; Gong, L. Long-lasting legacy of forest succession and forest management: Characteristics of coarse woody debris in an evergreen broad-leaved forest of Eastern China. *For. Ecol. Manag.* **2007**, *252*, 98–107.
28. Eaton, J.M.; Lawrence, D. Woody debris stocks and fluxes during succession in a dry tropical forest. *For. Ecol. Manag.* **2006**, *232*, 46–55.
29. Moseley, K.R.; Castleberry, S.B.; Ford, W.M. Coarse woody debris and pine litter manipulation effects on movement and microhabitat use of *Ambystoma talpoideum* in a *Pinus taeda* stand. *For. Ecol. Manag.* **2004**, *191*, 387–396.
30. Carmona, M.R.; Armesto, J.J.; Aravena, J.C.; Perez, C.A. Coarse woody debris biomass in successional and primary temperate forests in Chiloe Island, Chile. *For. Ecol. Manag.* **2002**, *164*, 265–275. [[CrossRef](#)]
31. Szymański, C.; Fontana, G.; Sanguinetti, J. Natural and anthropogenic influences on coarse woody debris stocks in *Nothofagus*—*Araucaria*, forests of northern Patagonia, Argentina. *Austral Ecol.* **2017**, *42*, 48–60. [[CrossRef](#)]
32. Kang, Y.X.; Cheng, Y.P. Woody plant flora of the Huoditang forest region. *J. Northwest For. Coll.* **1996**, *11*, 1–10, (In Chinese, with English abstract).
33. Harmon, M.E.; Sexton, J. *Guidelines for Measurements of Woody Debris in Forest Ecosystems*; US LTER Network Office, University of Washington: Seattle, WA, USA, 1996.
34. Ringvall, A.; Ståhl, G. Field aspects of line intersect sampling for assessing coarse woody debris. *For. Ecol. Manag.* **1999**, *119*, 163–170. [[CrossRef](#)]
35. Chen, C.G.; Peng, H. Standing crops and productivity of the major forest-types at the Huoditang forest region of the Qinling Mountains. *J. Northwest For. Coll.* **1996**, *11*, 92–102, (In Chinese, with English abstract).
36. Wenger, K.F. *Forestry Handbook*; John Wiley & Sons: New York, NY, USA, 1984.
37. Baker, T.R.; Honorio Coronado, E.N.; Phillips, O.L.; Martin, J.; van der Heijden, G.M.; Garcia, M.; Silva Espejo, J. Low stocks of coarse woody debris in a southwest Amazonian forest. *Oecologia* **2007**, *152*, 495–504. [[CrossRef](#)] [[PubMed](#)]
38. Fang, J.Y.; Liu, G.H.; Xu, S.L. Biomass and net production of forest vegetation in China. *Acta Ecol. Sin.* **1996**, *16*, 497–508, (In Chinese, with English abstract).
39. Hou, L.; Lei, R.D. Carbon dioxide sequestration of main shrub species in a natural secondary *Pinus tabulaeformis* forest at the Huoditang forest zone in the Qinling Mountains. *Acta Ecol. Sin.* **2009**, *29*, 6077–6084, (In Chinese, with English abstract).
40. Pang, H.D.; Wang, X.R.; Zhang, J.L.; Zheng, L.Y.; Cui, H.X. Characteristics of shrub layer biomass and carbon density in different forest types and different regions in Hubei province. *J. Northwest For. Univ.* **2014**, *29*, 46–51, (In Chinese, with English abstract).
41. Chen, H.; Harmon, M.E. Dynamic study of coarse woody debris in temperate forest ecosystem. *Chin. J. Appl. Ecol.* **1992**, *3*, 99–104, (In Chinese, with English abstract).
42. Muller, R.N.; Liu, Y. Coarse woody debris in an old-growth deciduous forest on the Cumberland plateau, southeastern Kentucky. *Can. J. For. Res.* **1991**, *21*, 1567–1572. [[CrossRef](#)]
43. Delaney, M.; Brown, S.; Lugo, A.E.; Torres-Lezama, A.; Bello Quintero, N. The quantity and turnover of dead wood in permanent forest plots in six life zones of Venezuela. *Biotropica* **1998**, *30*, 2–11. [[CrossRef](#)]
44. Nilsson, S.G.; Niklasson, M.; Hedin, J.; Aronsson, G.; Gutowski, J.M.; Linder, P.; Ljungberg, H.; Mikusiński, G.; Ranius, T. Densities of large living and dead trees in old-growth temperate and boreal forests. *For. Ecol. Manag.* **2002**, *161*, 189–204. [[CrossRef](#)]
45. Aakala, T.; Kuuluvainen, T.; Gauthier, S.; De Grandpré, L. Standing dead trees and their decay-class dynamics in the northeastern boreal old-growth forests of Quebec. *For. Ecol. Manag.* **2008**, *255*, 410–420. [[CrossRef](#)]
46. Pedlar, J.H.; Pearce, J.L.; Venier, L.A.; McKenney, D.W. Coarse woody debris in relation to disturbance and forest type in boreal Canada. *For. Ecol. Manag.* **2002**, *158*, 189–194. [[CrossRef](#)]
47. Aakala, T.; Kuuluvainen, T.; Grandpré, L.D.; Gauthier, S. Trees dying standing in the northeastern boreal old-growth forests of Quebec: Spatial patterns, rates, and temporal variation. *Can. J. For. Res.* **2006**, *37*, 50–61. [[CrossRef](#)]
48. Yuan, J.; Wei, X.; Shang, Z.C.; Cheng, F.; Hu, Z.Y.; Zheng, X.F.; Zhang, S.X. Impacts of CWD on understory biodiversity in forest ecosystems in the Qinling Mountains, China. *Pak. J. Bot.* **2015**, *47*, 1855–1864.
49. Keller, M.; Palace, M.; Asner, G.P.; Pereira, R.; Silva, J.N.M. Coarse woody debris in undisturbed and logged forests in the eastern Brazilian Amazon. *Glob. Chang. Biol.* **2004**, *10*, 784–795. [[CrossRef](#)]

50. Motta, R.; Berretti, R.; Lingua, E.; Piussi, P. Coarse woody debris, forest structure and regeneration in the Valbona Forest Reserve, Paneveggio, Italian Alps. *For. Ecol. Manag.* **2006**, *235*, 155–163. [[CrossRef](#)]
51. Li, L.H.; Dang, G.D. Coarse woody debris in an *Abies fargesii* forest in the Qinling Mountains. *Acta Phytoecol. Sin.* **1998**, *22*, 434–440, (In Chinese, with English abstract).
52. He, F.; Wang, D.X.; Zhang, S.Z.; Liu, W.Z.; Shen, Y.Z.; Hu, Y.N. Reserves of litter and woody debris of two main forests in the Xiaolong Mountains, Gansu, China. *Chin. J. Appl. Environ. Biol.* **2011**, *17*, 46–50, (In Chinese, with English abstract). [[CrossRef](#)]
53. Yuan, J.; Cheng, F.; Zhao, P.; Qiu, R.; Wang, L.; Zhang, S.X. Characteristics in coarse woody debris mediated by forest developmental stage and latest disturbances in a natural secondary forest of *Pinus tabulaeformis*. *Acta Ecol. Sin.* **2014**, *34*, 232–238. [[CrossRef](#)]
54. Harmon, M.E.; Chen, H. Coarse woody debris dynamics in two old growth ecosystems. *Bioscience* **1991**, *41*, 604–610. [[CrossRef](#)]
55. Li, L.H.; Xing, X.R.; Huang, D.M.; Liu, C.D.; He, J.Y. Storage and dynamics of coarse woody debris in *Castanopsis eyrei* forest of Wuyi Mountain, with some considerations for its ecological effects. *Acta Phytoecol. Sin.* **1996**, *20*, 132–143, (In Chinese, with English abstract).
56. Wang, R.L.; Yang, W.; Yang, Z.Z.; Chen, X.P.; Yang, C.P.; Li, Q.; Li, F.; Chen, C.M. Electroantennographic and behavioral responses of *Dendroctonus armandi* (Coleoptera: Ipsidae) to host plant volatiles. *Chin. J. Ecol.* **2011**, *30*, 724–729, (In Chinese, with English abstract).
57. Stevens, V. *The Ecological Role of Coarse Woody Debris: An Overview of the Ecological Importance of CWD in BC Forests*; Ministry of Forests, Research Program: Victoria, BC, Canada, 1997.
58. Sturtevant, B.R.; Bissonette, J.A.; Long, J.N.; Roberts, D.W. Coarse woody debris as a function of age, stand structure, and disturbance in boreal Newfoundland. *Ecol. Appl.* **1997**, *7*, 702–712. [[CrossRef](#)]
59. Spies, T.; Franklin, J.; Thomas, T. Coarse woody debris in Douglas-fir forests of western Oregon and Washington. *Ecology* **1988**, *69*, 1689–1702. [[CrossRef](#)]
60. Chambers, J.Q.; Higuchi, N.; Schimel, J.P.; Ferreira, L.V.; Melack, J.M. Decomposition and carbon cycling of dead trees in tropical forests of the central Amazon. *Oecologia* **2000**, *122*, 380–388. [[CrossRef](#)] [[PubMed](#)]
61. Brischke, C.; Rapp, A.O. Influence of wood moisture content and wood temperature on fungal decay in the field: Observations in different micro-climates. *Wood Sci. Technol.* **2008**, *42*, 663–677. [[CrossRef](#)]
62. He, D.J.; He, X.J.; Hong, W.; Qin, D.H.; Liu, J.S.; Cai, C.T. Quantitative characteristics of coarse woody debris in natural *Rhododendron simiarum* forests in Tianbaoyan National Nature Reserve. *J. Fujian Coll. For.* **2008**, *28*, 293–298, (In Chinese, with English abstract).



© 2017 by the authors. Licensee MDPI, Basel, Switzerland. This article is an open access article distributed under the terms and conditions of the Creative Commons Attribution (CC BY) license (<http://creativecommons.org/licenses/by/4.0/>).